OPEN ACCESS

# Journal of Orthopedic Research and Therapy

Leuzinger D, et al. J Orthop Res Ther 8: 1321.

www.doi.org/10.29011/2575-8241.001321

www.gavinpublishers.com

GAVIN PUBLISHERS

## Research Article

# A CT based 3D Algorithm for Diagnosis of DDH and Quantification of Surgical Correction

**David Leuzinger[1#], Armando Hoch[1*#], Philipp Fürnstahl[2], Patrick Zingg[1]**

[1]Department of Orthopedics, Balgrist University Hospital, University of Zurich, Zurich, Switzerland

[2]Research in Orthopaedic Computer Science, Balgrist University Hospital, University of Zurich, Zurich, Switzerland

[#]These authors contributed equally

***Corresponding Authors:** Armando Hoch, Department of Orthopaedics, Balgrist University Hospital, Forchstrasse 340, 8008 Zurich, Switzerland

**Citation:** Leuzinger D, Hoch A, Fürnstahl P, Zingg P (2023) A CT based 3D Algorithm for Diagnosis of DDH and Quantification of Surgical Correction. J Orthop Res Ther 8: 1321. DOI: 10.29011/2575-8241.001321

**Received Date:** 14 September, 2023; **Accepted Date:** 19 September, 2023; **Published Date:** 21 September, 2023

## Abstract

**Introduction:** Conventional radiographs are not doing justice to the complexity of 3D hip pathologies. Some methods based on 3D technology did not find their way to clinical practice. The goal of this study was to develop a 3D measurement method (named spidermap) for the acetabular coverage that can be used for the diagnosis of DDH as well as for the quantification of correction after Periacetabular Osteotomy (PAO).

**Methods:** In a first step we defined the threshold between physiological and dysplastic hips using this spidermap and in a second step we compared physiological to surgically treated dysplastic hips to quantify the correction. The population included three groups: Group A consisted of 18 physiological, group B of 21 dysplastic and group C of 8 surgically corrected hips. CT scans were used to calculate femoral head coverage by using the newly developed 3D algorithm. The result is a 2D map, a circular diagram showing anterior coverage at 0°, lateral coverage at 90°, posterior coverage at 180° and medial coverage at -90°. In a first step, groups A and B were compared to determine in which areas there was a significant threshold regarding coverage. In a second step groups A and C were compared to quantify the surgical correction after PAO.

**Results:** A significant threshold between groups A and B was found in the areas from -30° to 247.5° ($p < 0.05$). In the areas from 0° to 180° the specificity was high (>95%). The comparison of groups A and C showed a significant improvement in the areas from of 37° to 202.5° after PAO ($p < 0.05$).

**Conclusion:** Our 3D measurement method was able to reliably distinguish between physiological und dysplastic hips which allows for diagnosis of DDH in three dimensions. Furthermore, the spidermap allows for assessment of successful correction after PAO.

## Introduction

Developmental hip dysplasia is a common reason for hip pain in young adults and known to be a significant risk factor for secondary osteoarthritis [1]. Today the radiographic diagnosis of DDH in adults is based on multiple parameters that are measured on conventional radiographs. Each of those parameters focuses on a single aspect of the configuration of the hip joint. Summed up they allow an experienced orthopaedic surgeon to evaluate the hip joint as a whole. However, it is an attempt to describe a 3D problem with a 2D method. Furthermore, it is depending on multiple other variables such as the quality and technique of the radiograph and on the experience of the observer [2-4]. A 3D method to evaluate the configuration of a hip joint is highly desired. It would allow to see the hip joint as a whole, to carry out preoperative 3D error quantification, to serve as fundament for individual surgical planning and 3D computer assisted surgical guiding methods. A few studies using a similar 3D approach to our study already exist [5-9], but are rather two- than three-dimensional, are not covering acetabular deformities or did not look in the quantification of surgically corrected deformities. The goal of this study was to develop an illustrative 3D measurement method (spidermap) for the acetabular coverage that can be used for the diagnosis of DDH as well as for the quantification of correction after Periacetabular Osteotomy (PAO). Therefore, in a first step we defined the threshold between physiological and dysplastic hips using the novel spidermap and in a second step we compared physiological to surgically treated dysplastic hips to quantify the correction.

### Methods

### Patients

This study was approved by the local ethical committee (KEK ZH, BASEC Nr. 2018-01921). Three groups of patients were analyzed. Group A consisted of 18 hips in 10 patients (2 were excluded to previous surgery) with a physiological hip configuration. In all hips an anteroposterior (ap) pelvic radiograph and a CT scan of the pelvis was available. The patients were consecutive patients from our outpatient's clinic with the beforementioned imaging available. None of them showed radiographic signs of dysplasia (LCEA > 22°, ACI < 13°) [10] or had no history of hip pain). Group B consisted of young adults with dysplastic hips. In all hips an anteroposterior pelvic radiograph and a CT scan of the pelvis was available. Group C is a subset of Group B with patients who underwent PAO in out institution. In all hips an anteroposterior pelvic radiograph and a pre- and postoperative CT scan of the pelvis was available. All patients of Group B and C (consecutive series of patients) received the PAO in our institution. In Group C 3 hips were excluded after the surgery due to bad quality of the post-operative CT scan in certain areas of interest and consecutive processing error. Patient demographics and conventional radiographic parameters are available in Table 1.

| Groups | A | B | C |
|---|---|---|---|
| n | 18 | 21 | 8 |
| age [y] | 69 | 23 | 22 |
| m / f | 12-Jun | Jun-15 | 02-Jun |
| LCEA [°] (range) | 32 (22 - 45) | 16 (0 - 22) | |
| ACI [°] (range) | 2 (-10 - 12) | 14 (5 - 35) | |

**Table 1:** Demographic Data.

### Data Acquisition and Processing

Plain ap pelvic radiographs and CT scans of the pelvis of all patients were carried out (Group A) or already available (Group B and C). The radiographs were used to confirm the absence (Group A) or presence (Group B) of a DDH with conventional radiographic parameters (LCEA, ACI). The CT scans were used to generate 3D models. All CT scans were performed in our institution, using Siemens Definition AS® or Somatom Edge CT® scanners. Slice thickness was 1.0 mm with an in-plane resolution (x-y) of 0.4 x 0.4 mm. The CT scans were segmented and smoothened using the global thresholding and region growing functionality of a standard segmentation software (Mimics Medical 19, Materialise NV, Leuven, Belgium) to generate 3D bone models (Figure 1).

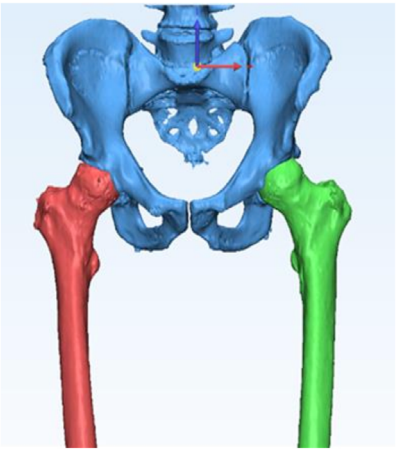

**Figure 1:** 3D bone model of pelvic bone (blue) and both femurs (red and green).

Our in-house developed software was used to process these models. The algorithm is based on a Matlab (Version R2015b, MathWorks, Natick, MA, USA) script. The models are standardized in their spatial orientation by calculating the anterior pelvic plane (APP) with help of the surgeon indicating the most anterior points of the anterior superior iliac spines and the pubic tubercles. Then the surgeon marks random surface points on the femoral heads

and the algorithm calculates a best fit sphere to define their centers (Figure 2). An axis through both centers is laid. Thereafter the limbus acetabuli is defined. Therefore, the surgeon marks random surface points on the acetabular rim. The algorithm uses these points to create an acetabular opening plane that is used to define the complete limbus acetabuli by minimal vertical distance to this predefined opening plane (Figure 3). The algorithm then calculates at total of 48 angles (comparable to the LCE angle) all around this axis. The angles measured are between the axis and a line drawn from the center of the femoral head of the joint assessed to its limbus acetabuli and each represents its local coverage according to Larson et al. [7] (Figure 4). This part of the processing is completely automated. These angles are then converted into percentage of coverage and presented on a spidermap. A 180° angle measured by the algorithm for local coverage corresponds to 100% coverage. The spidermap is a circular diagram, able to show the 3D data in 2D. The x-axis represents the rotation around the femoral head in degrees and the y-axis shows the percentage of femoral head coverage. For the spatial orientation 0° reflects anterior, 90° lateral, 180° posterior and -90° medial.

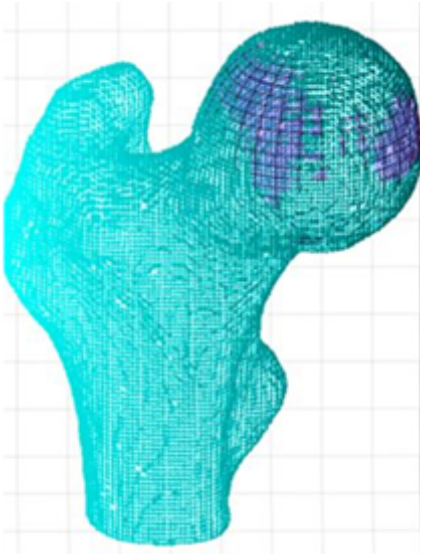

**Figure 2:** 3D bone model of proximal femur (turquoise) with best-fit sphere (blue) of femoral head for determination of center of rotation

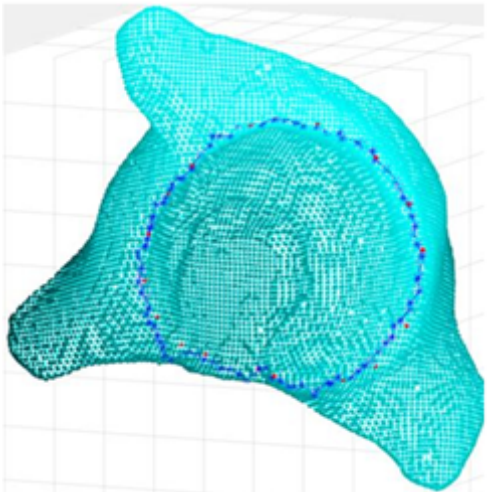

**Figure 3:** 3D bone model of acetabulum (turquoise) with limbus acetabuli marked with random points (red) and calculated opening plane (blue)

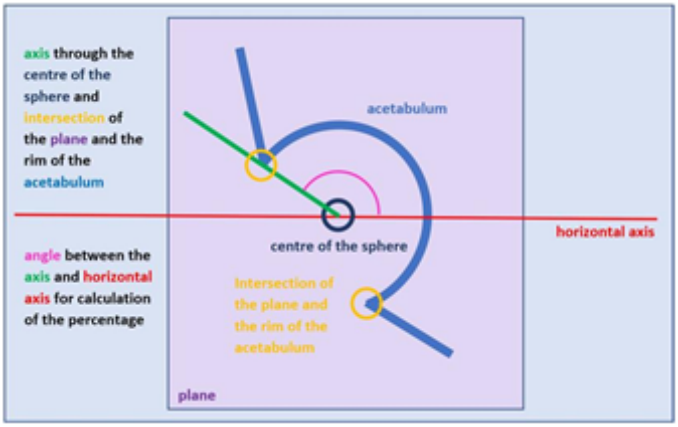


**Figure 4:** Illustration of different angles representing local coverage.

### Statistical Methods

For the first goal we defined the threshold, and the sensitivity and specificity for every of the 48 points of local coverage by calculating the ROC-curve using SPSS (SPSS Statistics 26, IBM, Armonk, New York, USA). By using the Youden-Index on the

ROC-curves, we were able to find the most precise threshold with its sensitivity and specificity. For the second goal we compared the coverage of the physiologic and the surgically corrected group by defining the average local coverage for all measuring points for both groups to plot a Spidermap and compared those measurements to each other by using a Mann-Whitney-U test using SPSS. A p-value of $< 0.05$ was considered as statistically significant.

## Results

A significant threshold between groups A and B was found in the area from -30° (anteromedial) to 247.5° (posteromedial) ($p < 0.05$) (bright blue and blue line with yellow glow). In the area from 0° (anterior) to 180° (posterior) the specificity was particularly high (>95%) (dark blue) (Figure 5). The comparison of groups A and C showed a successful improvement of the acetabular coverage in the area from of 37.5° (anterolateral) to 202.5° (posteromedial) in which there was no significant difference between the two groups (bright green). In the area of 52.5° (anterolateral) to 180° (posterior), the coverage of the hips of group C could even be raised above the threshold for a physiological hip (dark green) (Figure 6). The results are also delivered in Table 2 in numeric data.

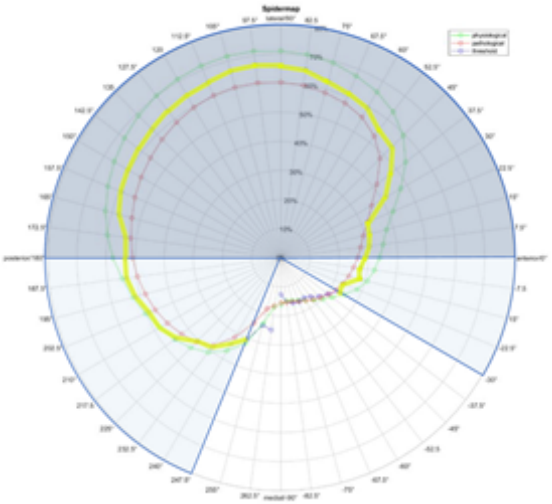

**Figure 5:** Spidermap showing areas of a significant difference (bright blue) between physiological (green) and dysplastic (red) hips, significant threshold is indicated with a yellow glow. Dark blue areas show a particularly high specificity.

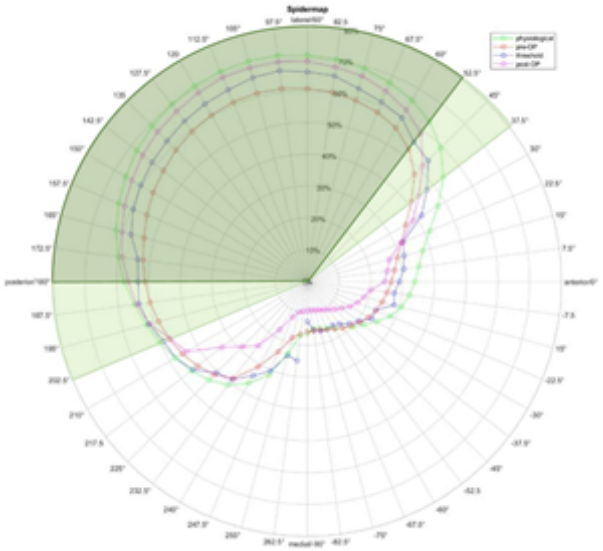

**Figure 6:** Spidermap showing areas of successful correction after PAO with no significant difference between the dysplastic and the postoperative group (bright green), in certain areas postoperative values were even raised above the threshold (dark green).

| Groups | | A (%) | | B (%) | | C (%) | | p-values | | Sensitivity (%) | Specificity (%) |
|---|---|---|---|---|---|---|---|---|---|---|---|
| Degree (°) / Localization | | mean | sd | mean | sd | mean | sd | A vs. B | A vs. C | | |
| -90 | medial | 16.1 | 3.67 | 15.51 | 2.88 | 8.6 | 3.06 | 0.908 | 0 | 14.3 | 100 |
| -82.5 | | 14.95 | 2.34 | 15.38 | 2.49 | 8.61 | 2.82 | 0.523 | 0 | 61.9 | 44.4 |
| -75 | | 15.12 | 2.78 | 15.58 | 2.34 | 8.81 | 2.75 | 0.706 | 0 | 66.7 | 44.4 |
| -67.5 | | 15.83 | 2.82 | 16.11 | 2.26 | 9.17 | 2.82 | 0.862 | 0 | 66.7 | 44.4 |
| -60 | | 16.86 | 2.97 | 16.97 | 2.35 | 9.71 | 3 | 0.75 | 0 | 47.6 | 77.8 |
| -52.5 | | 18.28 | 3.21 | 18.11 | 2.41 | 10.51 | 3.32 | 0.685 | 0 | 42.9 | 83.3 |
| -45 | | 20.15 | 3.64 | 19.36 | 2.48 | 11.69 | 3.76 | 0.367 | 0 | 47.6 | 83.3 |
| -37.5 | | 22.28 | 4.06 | 20.72 | 2.81 | 13.14 | 4.21 | 0.179 | 0 | 52.4 | 83.3 |
| -30 | | 25.16 | 4.1 | 21.9 | 3.19 | 15.01 | 3.91 | 0.019 | 0 | 76.2 | 72.2 |
| -22.5 | | 28.34 | 4.2 | 23.03 | 3.5 | 16.78 | 3.98 | 0 | 0 | 57.1 | 100 |
| -15 | | 30.72 | 4.26 | 24.17 | 3.53 | 18.02 | 3.88 | 0 | 0 | 90.5 | 77.8 |
| -7.5 | | 32.35 | 4.19 | 25.17 | 3.67 | 19.87 | 3.48 | 0 | 0 | 81 | 100 |
| 0 | anterior | 33.83 | 4.19 | 26.37 | 3.97 | 24.75 | 6.8 | 0 | 0.001 | 81 | 100 |
| 7.5 | | 35.41 | 4.9 | 27.66 | 4.31 | 25.4 | 5.47 | 0 | 0.001 | 81 | 100 |
| 15 | | 37.59 | 6.14 | 29.28 | 4.9 | 26.52 | 7.83 | 0 | 0.001 | 71.4 | 100 |
| 22.5 | | 41.67 | 8.45 | 32.24 | 5.96 | 31.6 | 8.46 | 0 | 0.004 | 61.9 | 100 |

| | | | | | | | | | | | |
|---|---|---|---|---|---|---|---|---|---|---|---|
| 30 | | 47.48 | 8.14 | 35.95 | 7.34 | 37 | 10.96 | 0 | 0.041 | 76.2 | 83.3 |
| 37.5 | | 53.97 | 6.86 | 41.52 | 8.67 | 43.18 | 11.88 | 0 | 0.08 | 71.4 | 88.9 |
| 45 | | 59.38 | 5.25 | 48.27 | 7.31 | 50.31 | 11.69 | 0 | 0.115 | 81 | 88.9 |
| 52.5 | | 63.28 | 4.82 | 52.68 | 5.82 | 58.32 | 5.24 | 0 | 0.054 | 81 | 100 |
| 60 | | 65.86 | 4.68 | 55.75 | 4.89 | 62.2 | 3.54 | 0 | 0.115 | 85.7 | 94.4 |
| 67.5 | | 67.63 | 4.78 | 57.51 | 4.78 | 64.97 | 2.42 | 0 | 0.285 | 85.7 | 94.4 |
| 75 | | 69.34 | 4.58 | 58.68 | 4.85 | 67.11 | 1.86 | 0 | 0.429 | 85.7 | 100 |
| 82.5 | | 70.37 | 4.43 | 59.71 | 4.61 | 68.11 | 1.5 | 0 | 0.461 | 95.2 | 94.4 |
| 90 | lateral | 71.1 | 4.43 | 60.27 | 4.3 | 69.23 | 0.88 | 0 | 0.935 | 95.2 | 94.4 |
| 97.5 | | 71.58 | 4.55 | 60.64 | 4.16 | 69.53 | 1.02 | 0 | 0.807 | 100 | 94.4 |
| 105 | | 71.64 | 4.61 | 60.64 | 4.14 | 69.37 | 1.37 | 0 | 0.567 | 100 | 94.4 |
| 112.5 | | 71.39 | 4.77 | 60.35 | 4.1 | 69.24 | 1.64 | 0 | 0.605 | 100 | 100 |
| 120 | | 70.94 | 5.08 | 59.67 | 3.94 | 68.34 | 2.12 | 0 | 0.367 | 95.2 | 100 |
| 127.5 | | 70.19 | 5.13 | 58.68 | 3.84 | 67.37 | 2.69 | 0 | 0.261 | 95.2 | 100 |
| 135 | | 69.05 | 5.32 | 57.57 | 3.74 | 66.54 | 2.78 | 0 | 0.367 | 95.2 | 100 |
| 142.5 | | 67.6 | 5.36 | 56.38 | 3.62 | 65.25 | 2.95 | 0 | 0.495 | 95.2 | 94.4 |
| 150 | | 65.99 | 5.16 | 55.32 | 3.52 | 63.44 | 3.17 | 0 | 0.216 | 95.2 | 94.4 |
| 157.5 | | 64.21 | 4.76 | 54.19 | 3.54 | 61.92 | 3.48 | 0 | 0.261 | 95.2 | 94.4 |
| 165 | | 62.26 | 4.51 | 52.91 | 3.23 | 59.88 | 3.61 | 0 | 0.216 | 95.2 | 94.4 |
| 172.5 | | 60.02 | 4.57 | 51.9 | 3.16 | 58.1 | 3.32 | 0 | 0.338 | 81 | 100 |
| 180 | posterior | 57.61 | 4.33 | 50.86 | 3.21 | 55.22 | 3.8 | 0 | 0.16 | 85.7 | 88.9 |
| 187.5 | | 54.84 | 4.36 | 49.6 | 3.17 | 53.01 | 4.3 | 0 | 0.285 | 95.2 | 66.7 |
| 195 | | 52.45 | 3.85 | 48.13 | 3.39 | 49.93 | 4.49 | 0 | 0.177 | 90.5 | 66.7 |
| 202.5 | | 50.19 | 3.5 | 46.66 | 3.42 | 44.64 | 10.5 | 0.006 | 0.08 | 81 | 61.1 |
| 210 | | 47.89 | 3.5 | 44.88 | 3.42 | 41.84 | 8.98 | 0.011 | 0.022 | 85.7 | 55.6 |
| 217.5 | | 45.93 | 3.48 | 42.96 | 3.32 | 29.83 | 17.27 | 0.01 | 0.003 | 81 | 66.7 |
| 225 | | 43.66 | 3.74 | 40.85 | 3.41 | 27.18 | 15.36 | 0.036 | 0.002 | 61.9 | 83.3 |
| 232.5 | | 40.91 | 3.75 | 37.91 | 3.83 | 24.5 | 13.99 | 0.026 | 0.001 | 57.1 | 66.7 |
| 240 | | 36.81 | 5.75 | 31.48 | 7.7 | 17.21 | 11.44 | 0.015 | 0 | 57.1 | 83.3 |
| 247.5 | | 31.77 | 6.41 | 24.24 | 7.3 | 11.67 | 5.81 | 0.003 | 0 | 85.7 | 72.2 |
| 255 | | 23.41 | 8.44 | 18.09 | 4.36 | 9.36 | 3.78 | 0.17 | 0 | 85.7 | 44.4 |
| 262.5 | | 16.96 | 4.8 | 16.56 | 3.61 | 8.86 | 3.31 | 0.816 | 0 | 100 | 16.7 |

**Table 2:** Algorithm Data.

## Discussion

We have developed an algorithm which allows to generate a 2D map of the acetabular coverage using 3D CT data that does justice to the three-dimensionality of DDH. The algorithm allows circumferential quantification of the acetabular coverage and thus also permits precise localization of a diminished coverage. We contrasted physiologic and dysplastic hips and determined a threshold value for each area around the acetabular hemisphere. This was significant between the collectives. Thus, the algorithm can provide reliable help in the diagnosis of DDH on the basis of 3D data. Due to the easy visualization of the algorithm with the spidermap, an illustration of the coverage is possible, which can help the surgeon to consult patients and to plan a surgical correction. Furthermore, we were able to quantify the correction of the dysplastic hips by means of the PAO using the algorithm. Successful correction was shown in our collective. In particular, the correction within the biomechanically relevant anterolateral part of the joint was very good, so that the coverage could be raised above the threshold for a normal hip [8].

Some authors have also dealt with this topic and gained relevant insights into the three-dimensionality of DDH. As a result, various suggestions were made regarding possibilities in diagnostics and preoperative planning, which are briefly discussed below. Murphy et al. in 1990 set the milestone for the understanding of the three-dimensionality in DDH by showing in a 3D analysis that the dysplasia of the hip is not a malorientation of the acetabulum, but rather a globally insufficient coverage [8]. Janzen et al. formulated the idea of measuring the coverage at different locations of the acetabulum on CT and thus used the same data basis as we did [6]. However, the measurements were taken manually and in individual two-dimensional slices of the CT. The same group used a similar method to quantify the result of surgically corrected dysplastic hips as we did, but with the same disadvantages of their supposedly three-dimensional method [5]. Two studies assessed the differences in normal and dysplastic hips using volumetric quantification of the femoral head or the acetabulum. Miyasaka et al. calculated the volume of the covered femoral head and stated that in dysplastic hips only half the volume compared to normal hips was covered [11]. Van Bosse et al. deducted a study calculating the volume of the acetabular space [9]. Their key message was that the dysplastic acetabulum was shallower in depth and elongated cranio-caudally. They as well found no significant anteversion in dysplastic compared to normal hips. Like most of the studies mentioned above, these volume dependent studies lack a illustrative presentation of the assessment of a hip configuration and a dedicated spatial resolution. Larson et al. published a study that attempted to simplify the three-dimensional anatomy of the acetabulum using a similar methodology that we sed [7]. This study examined only the normal anatomy without addressing various patterns of deformity or their correction.

To our knowledge, there is no study to date that allows automated quantification of acetabular coverage based on 3D data and uses this to calculate a locally precise resolution of the deformity. Furthermore, no comparison has yet been made between physiological and dysplastic, let alone surgically corrected hips using a 3D-based measurement method. This study is thus the first to investigate this. It can be taken as a basis for refining the three-dimensional understanding of DDH. This is imperative in the consultation and treatment of patients, especially since current diagnostic methods and also surgical planning do not do justice to the three-dimensional problem. In the future, it should be possible to carry out three-dimensional corrections precisely with the aid of computer-assisted technologies. This is only possible when the fundamental knowledge of the pathology in three dimensions, as well as corresponding planning possibilities, are available. Our method must be refined for this purpose: The calculated threshold is based on the combination of the known conventional parameters for hip dysplasia and does not represent a novel independent diagnostic approach. Once the understanding of the problem has been extended, the diagnosis can be made fully on three-dimensional data. New diagnostic criteria would be the logical consequence.The study has its limitations. The algorithm is partially automated, so errors may occur if the image quality is poor. Although these can be corrected manually, the claim for the method is that this is not necessary. Nevertheless, there is no clinical relevance, especially since the errors occur in the posteromedial area where the algorithm misinterprets the ischial bone as acetabular rim. Furthermore, although the femoral head center was used for the algorithm, femoral torsion was not. This, combined with the fact that the data set was collected with the patient in the supine position, means that functional aspects were not considered when calculating the coverage. The clear advantage of our method lies in the fact, that we are able to facilitate the diagnosis of DDH based upon standardized 3D information, analyzing and displaying it on an easy to understand spidermap and reading the optimal amount and direction for operative correction through PAO directly from the map. The next step will be to use this knowledge for the three-dimensionally planned correction and its execution.

## Conclusion

The introduced 3D measurement method was able to reliably distinguish between physiological und dysplastic hip configurations which allows for diagnosis of DDH in three dimensions. Furthermore, the spidermap allows for assessment of successful correction after PAO.

## References

1. Jacobsen S, Sonne-Holm S (2005) Hip dysplasia: a significant risk factor for the development of hip osteoarthritis. A cross-sectional survey. Rheumatology (Oxford) 44: 211-218.
2. Kalberer F, Sierra RJ, Madan SS, Ganz R, Leunig M (2008) Ischial spine projection into the pelvis : a new sign for acetabular retroversion. Clin Orthop Relat Res 466: 677-683.
3. Clohisy JC, Carlisle JC, Trousdale R, Kim YJ, Beaule PE, et al. (2009) Radiographic evaluation of the hip has limited reliability. Clin Orthop Relat Res 467: 666-675.
4. Malviya A, Raza A, Witt JD (2016) Reliability in the diagnosis of femoroacetabular impingement and dysplasia among hip surgeons: role of surgeon volume and experience. Hip Int 26: 284-289.
5. Haddad FS, Garbuz DS, Duncan CP, Janzen DL, Munk PL (2000) CT evaluation of periacetabular osteotomies. J Bone Joint Surg Br 82: 526-531.
6. Janzen DL, Aippersbach SE, Munk PL, Sallomi DF, Garbuz D, et al. (1998) Three-dimensional CT measurement of adult acetabular dysplasia: technique, preliminary results in normal subjects, and potential applications. Skeletal Radiol 27: 352-358.
7. Larson CM, Moreau-Gaudry A, Kelly BT, Byrd JW, Tonetti J, et al. (2015) Are normal hips being labeled as pathologic? A CT-based method for defining normal acetabular coverage. Clin Orthop Relat Res 473: 1247-1254.
8. Murphy SB, Kijewski PK, Millis MB, Harless A (1990) Acetabular dysplasia in the adolescent and young adult. Clin Orthop Relat Res 1990: 214-223.
9. van Bosse H, Wedge JH, Babyn P (2015) How are dysplastic hips different? A three-dimensional CT study. Clin Orthop Relat Res 473: 1712-1723.
10. Tannast M, Hanke MS, Zheng G, Steppacher SD, Siebenrock KA (2015) What are the radiographic reference values for acetabular under- and overcoverage? Clin Orthop Relat Res 473: 1234-1246.
11. Miyasaka D, Ito T, Imai N, Suda K, Minato I, et al. (2014) Three-dimensional Assessment of Femoral Head Coverage in Normal and Dysplastic Hips: A Novel Method. Acta Med Okayama 68: 277-284.